Synthesis, Structures, and Redox Properties of Octa(μ_3-sulfido)hexarhenium(III) Complexes Having Terminal Pyridine Ligands

Takashi Yoshimura,[†] Keisuke Umakoshi,[†] Yoichi Sasaki,*[,†] and A. Geoffrey Sykes[‡]

Graduate School of Science, Division of Chemistry, Hokkaido University, Kita-ku, Sapporo 060-0810, Japan, and Department of Inorganic and Structural Chemistry, The University of Newcastle, Newcastle-upon-Tyne NE1 7RU, U.K.

Received July 2, 1999

A series of μ_3-sulfido Re−Re bonded octahedral hexarhenium(III) clusters having mixed chloride−pyridine (py) or −4-cyanopyridine (cpy) terminal ligands, $[Bu_4N]_2$[*trans*-$\{Re_6S_8Cl_4(py)_2\}$] (Bu_4N^+ = tetra-*n*-butylammonium cation) (**1a**), $[Bu_4N]_2$[*cis*-$\{Re_6S_8Cl_4(py)_2\}$] (**1b**), $[Bu_4N]_2$[*trans*-$\{Re_6S_8Cl_4(cpy)_2\}$] (**2a**), $[Bu_4N]_2$[*cis*-$\{Re_6S_8Cl_4(cpy)_2\}$] (**2b**), and $[Bu_4N]$[*mer*-$\{Re_6S_8Cl_3(py)_3\}$] (**3**), and their one-electron-oxidized $Re^{III}_5Re^{IV}$ species, $[Bu_4N]$[*trans*-$\{Re_6S_8Cl_4(py)_2\}$] (**1a′**), $[Bu_4N]$[*trans*-$\{Re_6S_8Cl_4(cpy)_2\}$] (**2a′**), and *mer*-$[Re_6S_8Cl_3(py)_3]$ (**3′**), have been prepared and characterized by several physical methods. X-ray crystallographic studies for **1a**, **2a**, and **3** showed that the Re_6S_8 core structures are not significantly affected by the type and number of pyridyl ligands. The mixed valent cluster **1a′** is of a structurally delocalized type, structural parameters being very similar to those of **1a**. Cyclic voltammograms in acetonitrile showed that there is no distinct difference in the redox potentials (Re^{III}_6/$Re^{III}_5Re^{IV}$) between the cis and the corresponding trans isomers. Both **1a** and **1b** show a reversible redox wave at 0.77 V vs Ag/AgCl. Redox potentials are more positive for **2a** and **2b** (0.83 V) and **3** (0.97 V). Clusters **2a** and **2b** show two-step ligand-centered redox waves at −1.19 and −1.28 V, and −1.18 and −1.29 V, respectively. Temperature-dependent magnetic susceptibility measurements have revealed that **1a′** and **3′** have an $S = 1/2$ ground state. The electron self-exchange rate constant for the reaction of **2a** with **2a′** in dichloromethane as obtained by ^{1}H NMR line-broadening method is 1.2×10^9 M^{-1} s^{-1} (298.2 K) with $\Delta H^{\ddagger} = 30.2 \pm 2.1$ kJ mol^{-1} and $\Delta S^{\ddagger} = 30 \pm 8$ J mol^{-1} K^{-1}. It has been suggested that the previously reported protonated species $[Re_6S_7(SH)Cl_6]^{3-}$ would actually be a one-electron-oxidized $[Re_6S_8Cl_6]^{3-}$. Crystal data: $[Bu_4N]_2$[*trans*-$\{Re_6S_8Cl_4(py)_2\}$] (**1a**), monoclinic, space group *C*2/*c*, $a = 24.693(8)$ Å, $b = 19.494(4)$ Å, $c = 18.592(4)$ Å, $\beta = 115.76(2)°$, $Z = 4$; $[Bu_4N]_2$[*trans*-$\{Re_6S_8Cl_4(cpy)_2\}$] (**2a**), orthorhombic, space group *Cmca*, $a = 19.304(3)$ Å, $b = 17.894(7)$ Å, $c = 18.773(4)$ Å, $Z = 4$; $[Bu_4N]$[*mer*-$\{Re_6S_8Cl_3(py)_3\}$] (**3**), monoclinic, space group $P2_1/n$, $a = 16.156(5)$ Å, $b = 19.760(5)$ Å, $c = 18.895(4)$ Å, $\beta = 108.94(2)°$, $Z = 4$; $[Bu_4N]$[*trans*-$\{Re_6S_8Cl_4(py)_2\}$] (**1a′**), monoclinic, space group *C*2/*c*, $a = 20.524(5)$ Å, $b = 13.794(4)$ Å, $c = 16.399(4)$ Å, $\beta = 109.72(2)°$, $Z = 4$.

Introduction

The octahedral structural motif M_6X_8, where M is a metal ion and X is a chalcogenide or a halide ion capping the face of each metal triangle of the M_6 core, is now well-known as one of the most common cluster structural units.[1−10] The units are usually coordinated by six terminal ligands (L) to complete the octahedral cluster as $M_6X_8L_6$. Among the compounds having this structural unit, molybdenum and tungsten clusters have been the most extensively studied. The extended solid materials $M'_xMo_6S_8$ (M′ = alkali metal ions, alkaline earth metal ions, etc.) called Chevrel's phase are well-known for their superconducting behavior.[11] Discrete molecular compounds have also been prepared to study structural characteristics and chemical and physical properties. While chalcogenide-capped clusters are redox active,[12] the halogeno-capped forms are known for their photoluminescent properties.[10,13−24] Attempts have been made

[†] Hokkaido University.
[‡] The University of Newcastle.

(1) Lee, S. C.; Holm, R. H. *Angew. Chem., Int. Ed. Engl.* **1990**, *29*, 840−856.
(2) Dance, I.; Fisher, K. *Prog. Inorg. Chem.* **1994**, *41,* 637−803.
(3) Saito, T. *Early Transition Metal Clusters with π-Donor Ligands*; VCH: New York, 1995; pp 63−164.
(4) Saito, T. *Adv. Inorg. Chem.* **1996**, *44,* 45−91.
(5) Saito, T.; Imoto, H. *Bull. Chem. Soc. Jpn.* **1996**, *69*, 2403−2417.
(6) Bencini, A.; Biani, F. F.; Uyttrrhoeven, M. G. *Inorg. Chim. Acta* **1996**, *244*, 231−237 and references therein.
(7) Cecconi, F.; Ghiardi, C. A.; Midollini, S.; Orlandini, A.; Bencini, A. *J. Chem. Soc., Dalton Trans.* **1996**, 3991−3994 and references therein.
(8) Ogino, H.; Inomata, S.; Tobita, H. *Chem. Rev.* **1998**, *98*, 2093-2121 and references therein.
(9) Saito, T. *J. Chem. Soc., Dalton Trans.* **1999**, 97−105.
(10) Prokopuk, N.; Shriver, D. F. *Adv. Inorg. Chem.* **1999**, *46*, 1−49.
(11) Chevrel, R.; Hirrien, M.; Sergent, M. *Polyhedron* **1986**, *5,* 87−94.
(12) Saito, T.; Yamamoto, N.; Nagase, T.; Tsuboi, T.; Kobayashi, K.; Yamagata, T.; Imoto, H.; Unoura, K. *Inorg. Chem.* **1990**, *29*, 764−770.
(13) Maverick, A. W.; Gray, H. B. *J. Am. Chem. Soc.* **1981**, *103*, 1298−1300.
(14) Maverick, A. W.; Najdionek, J. S.; MacKenzie, D.; Nocera, D. G.; Gray, H. B. *J. Am. Chem. Soc.* **1983**, *105*, 1878−1882.
(15) Tanaka, H. K.; Sasaki, Y.; Saito, K. *Sci. Pap. Inst. Phys. Chem. Res.* **1984**, *78*, 92−96.
(16) Saito, Y.; Tanaka, H. K.; Sasaki, Y.; Azumi, T. *J. Phys. Chem.* **1985**, *89*, 4413−4415.
(17) Zietlow, T. C.; Nocera, D. G.; Gray, H. B. *Inorg. Chem.* **1986**, *25*, 5, 1351−1353.
(18) Zietlow, T. C.; Schaefer, W. P.; Sadeghi, B.; Nocera, D. G.; Gray, H. B. *Inorg. Chem.* **1986**, *25*, 2198−2201.
(19) Azumi, T.; Saito, Y. *J. Phys. Chem.* **1988**, *92*, 1715−1721.
(20) Mussell, R. D.; Nocera, D. G. *J. Am. Chem. Soc.* **1988**, *110*, 0, 2764−2772.
(21) Kraut, B.; Ferraudi, G. *Inorg. Chem.* **1989**, *28*, 4578−4583.

10.1021/ic9907922 CCC: $18.00
Published on Web 11/06/1999

to prepare finely tuned molecules having mixed chalcogenido−halogeno-capped cluster units[10,25−29] and complexes with various combinations of terminal ligands.[10] However, for the molybdenum and tungsten clusters, the preparation of different terminal ligand combinations in a controlled manner has not been achieved in a systematic way. Two mixed terminal phosphine complexes are known, namely, $Mo_6S_8(NO)(PEt_3)_5$[30] and $Mo_{12}S_{16}(PEt_3)_5$,[31] which have been prepared by substitution of PEt_3 on the starting material $Mo_6S_8(PEt_3)_6$. $Cr_{12}S_{16}(PEt_3)_5$ has been reported recently.[32] Di- and trisubstituted halogeno-capped clusters $[Mo_6Cl_8Cl_4X_2]^{n-}$ ($n = 0$, X = DMF, DMSO,[33] PEt_3;[34,35] $n = 2$, X = OCH_3, $OCH_2C_{14}H_9$)[36] and $[Mo_6Cl_8Cl_3(PEt_3)_3]^-$,[25] respectively, are also known.

Hexanuclear rhenium clusters with chalcogenido caps (S, Se, Te) are the most recently developed among the complexes with the hexanuclear motifs.[9,37−49] In addition to the discrete hexarhenium clusters, dimeric, oligomeric, and extended solid hexarhenium clusters are known. Mixed capped complexes of the combinations S−Te,[50] Se−Te,[43] S−Cl,[51,52] Se−Cl,[52−56] S−Br,[57] S−Se−Cl,[58] S−Te−Cl,[58] S−O−Cl,[59] Se−O−Cl,[54] S−Cl−NR, and Se−Cl−NR[60] have been prepared. Preparation of mixed terminal ligand complexes with the general formula $[Re_6S_8X_n(PR_3)_{6-n}]^{(n-2)-}$ ($n = 0-4$) and the μ_3-Se analogues indicate that the stepwise substitution of terminal halogeno ligands is possible for the hexarhenium clusters.[42,44] The clusters generally show reversible one-electron oxidation in their cyclic voltammograms.[38,41] Protonated derivatives with structural units $[Re_6S_7(SH)X_6]^{3-}$ (X = Cl, Br, I) and $[Re_6Se_7(SeH)I_6]^{3-}$ have been reported.[38] Very recently, photoluminescent properties of some hexarhenium clusters have been reported,[61] which reinforces the versatility of hexarhenium clusters.

Most studies of Re_6S_8 and Re_6Se_8 clusters to date deal with terminal halide, phosphine, cyanide, and solvent molecules as ligands. Only the hexarhenium cluster containing terminal pyridine (py) ligand is $[cis\text{-}\{Re_6Se_8(PEt_3)_4(py)_2\}]^{2+}$.[41] If pyridine type ligands can be successively introduced into the terminal sites of the hexanuclear units, control of chemical and physical properties of the hexarhenium clusters is far more promising by changing the basicities of pyridine derivatives and introducing functional substituents. A recent report on the dendrimers based on the coordination of pyridyl moieties at the Re_6Se_8 center has shown that such an approach is certainly promising.[49] Furthermore, seemingly substitution inert properties of the terminal sites as verified by the phosphine ligand substitution would enable us to control the ligand combinations of the terminal coordination sphere of the hexarhenium clusters.

In this paper we report the preparation and properties of mixed terminal ligand complexes $[Re_6S_8Cl_{6-n}(L)_n]^{(4-n)-}$ (L = py, $n = 2-4$; L = 4-cyanopyridine (cpy), $n = 2$) including trans and cis geometrical isomers for $n = 2$. We have also prepared and unambiguously characterized one-electron-oxidized species of these complexes. Our results seem to show that previously reported protonated species[38] would be one-electron-oxidized derivatives. The electron self-exchange rate has been estimated by using the redox pair of the hexarhenium clusters.

Experimental Section

Materials. $[Bu_4N]_3[Re_6S_8Cl_6]$ (Bu_4N^+ = tetra(*n*-butyl)ammonium ion) was prepared as described in the literature, in which the compound was claimed to be $[Bu_4N]_3[Re_6S_7(SH)Cl_6]$.[38] Acetonitrile was dried over calcium hydride and distilled under argon atmosphere. Tetrabutylammonium hexafluorophosphate ($(Bu_4N)PF_6$) was recrystallized twice from ethanol. All other commercially available reagents were used as supplied.

Preparation of the Complexes. $[Bu_4N]_2[$*trans*-$\{Re_6S_8Cl_4(py)_2\}]$ (1a) and $[Bu_4N]_2[$*cis*-$\{Re_6S_8Cl_4(py)_2\}]$ (1b). $[Bu_4N]_3[Re_6S_8Cl_6]$ (0.300 g, 0.13 mmol) and pyridine (0.205 g, 2.6 mmol) were dissolved in 60 mL of DMF. The solution was refluxed for 1 h, and was evaporated to ca. 5 mL under reduced pressure. On addition of 20 mL of water, a yellow-orange precipitate was formed, which was collected by filtration. The solid was dissolved in dichloromethane, and the solution was chromatographed on a silica gel column to obtain the two geometric isomers. A yellow band was held at the top of the column. The first fraction contained *mer*-$[Re_6S_8Cl_3(py)_3]^-$ in only small amounts.

(22) Tanaka, H. K.; Sasaki, Y.; Ebihara, M.; Saito, K. *Inorg. Chim. Acta* **1989**, *161*, 63−66.
(23) Mussell, R. D.; Nocera, D. G. *Inorg. Chem.* **1990**, *29*, 3711−3717.
(24) Mussell, R. D.; Nocera, D. G. *J. Phys. Chem.* **1991**, *95*, 6919−6924.
(25) Michel, J. B.; McCarley, R. E. *Inorg. Chem.* **1982**, *21*, 1864−1872.
(26) Ebihara, M.; Toriumi, K.; Saito, K. *Inorg. Chem.* **1988**, *27*, 13−18.
(27) Ebihara, M.; Isobe, K.; Sasaki, Y.; Saito, K. *Inorg. Chem.* **1992**, *31*, 1644−1649.
(28) Zhang, X.; McCarley, R. E. *Inorg. Chem.* **1995**, *34*, 2678−2683.
(29) Xie, X.; McCarley, R. E. *Inorg. Chem.* **1997**, *36*, 4011−4016.
(30) Mizutani, J.; Amari, S.; Imoto, H.; Saito, T. *J. Chem. Soc., Dalton Trans.* **1998**, 819−824.
(31) Amari, S.; Imoto, H.; Saito, T. *Chem. Lett.* **1997**, 967−968.
(32) Kamiguchi, S.; Imoto, H.; Saito, T. *Chem. Lett.* **1996**, 555−556.
(33) Cotton, F. A.; Curtis, N. F. *Inorg. Chem.* **1965**, *4*, 241−244.
(34) Saito, T.; Nishida, M.; Yamagata, T.; Yamagata, Y.; Yamaguchi, Y. *Inorg. Chem.* **1986**, *25*, 1111−1117.
(35) Ehrlich, G. M.; Warren, C. J.; Haushalter, R. C.; DiSalvo, F. J. *Inorg. Chem.* **1995**, *34*, 4284−4286.
(36) Perchenek, N.; Simon, A. *Z. Anorg. Allg. Chem.* **1993**, *619*, 98−102.
(37) Long, J. R.; Williamson, A. S.; Holm, R. H. *Angew. Chem., Int. Ed. Engl.* **1995**, *34*, 226−229.
(38) Long, J. R.; McCarty, L. S.; Holm, R. H. *J. Am. Chem. Soc.* **1996**, *118*, 4603−4616.
(39) Mironov, Y. V.; Pell, M. A.; Ibers, J. A. *Angew. Chem., Int. Ed. Engl.* **1996**, *35*, 2854−2856.
(40) Mironov, Y. V.; Pell, M. A.; Ibers, J. A. *Inorg. Chem.* **1996**, *35*, 2709−2710.
(41) Zheng, Z.; Holm, R. H. *Inorg. Chem.* **1997**, *36*, 5173−5178.
(42) Zheng, Z.; Long, J. R.; Holm, R. H. *J. Am. Chem. Soc.* **1997**, *119*, 2163-2171.
(43) Mironov, Y. V.; Cody, J. A.; Albrecht-Schmitt, T. E.; Pell, M. A.; Ibers, J. A. *J. Am. Chem. Soc.* **1997**, *119*, 493−498.
(44) Willer, M. W.; Long, J. R.; McLauchlan, C. C.; Holm, R. H. *Inorg. Chem.* **1998**, *37*, 328−333.
(45) Naumov, N. G.; Virovets, A. V.; Sokolov, M. N.; Artemkina, S. B.; Fedorov, V. E. *Angew. Chem., Int. Ed. Engl.* **1998**, *37*, 1943−1945.
(46) Beauvais, L. G.; Shores, M. P.; Long, J. R. *Chem. Mater.* **1998**, *10*, 3783−3786.
(47) Shores, M. P.; Beauvais, L. G.; Long, J. R. *J. Am. Chem. Soc.* **1999**, *121*, 775−779.
(48) Shores, M. P.; Beauvais, L. G.; Long, J. R. *Inorg. Chem.* **1999**, *38*, 1648−1649.
(49) Wang, R.; Zheng, Z. *J. Am. Chem. Soc.* **1999**, *121*, 3549−3550.
(50) Mironov, Y. V.; Virovets, A. V.; Fedorov, V. E.; Podberezskaya, N. V.; Shishkin, O. V.; Struchkov, Y. T. *Polyhedron* **1995**, *14*, 3171−3173.
(51) Gabriel, J.-C.; Boubekeur, K.; Batail, P. *Inorg. Chem.* **1993**, *32*, 2894−2900.
(52) Dolbecq, A.; Boubekeur, K.; Batail, P.; Canadell, E.; Auban-Senzier, P.; Coulon, C.; Lerstrup, K.; Bechgaard, K. *J. Mater. Chem.* **1995**, *5*, 1707−1718.
(53) Perrin, A. *New J. Chem.* **1990**, *14*, 561−567.
(54) Yaghi, O. M.; Scott, M. J.; Holm, R. H. *Inorg. Chem.* **1992**, *31*, 4778−4784.
(55) Penicaud, A.; Boubeker, K.; Batail, P.; Canadell, E.; Auban-Senzier, P.; Jerome, D. *J. Am. Chem. Soc.* **1993**, *115*, 4101−4112.
(56) Dolbecq, A.; Fourmigue, M.; Batail, P. *Bull. Soc. Chim. Fr.* **1996**, *133*, 83−88.
(57) Fedin, V. P.; Imoto, H.; Saito, T.; Fedorov, V. E.; Mironov, Y. V.; Yarovoi, S. S. *Polyhedron* **1996**, 1229−1233.
(58) Uriel, S.; Boubeker, K.; Batail, P.; Orduna, J.; Canadell, E. *Inorg. Chem.* **1995**, *34*, 5307−5313.
(59) Simon, F.; Boubekeur, K.; Gabriel, J.-C. P.; Batail, P. *Chem. Commun.* **1998**, 845−846.
(60) Uriel, S.; Boubeker, K.; Batail, P.; Orduna, J. *Angew. Chem., Int. Ed. Engl.* **1996**, *35*, 1544−1547.
(61) Yoshimura, T.; Ishizaka, S.; Umakoshi, K.; Sasaki, Y.; Kim, H.-B.; Kitamura, N. *Chem. Lett.* **1999**, 697−698.

The second yellow-orange band was collected by eluting with 1:20 acetonitrile/dichloromethane, and the eluate was left for several days to allow for evaporation in air. The yellow-orange solid deposited was filtered off, washed with water and a mixture of acetone and ether, and then dried in vacuo. Yield of the trans isomer **1a**: 0.069 g (28%). Anal. Calcd for $C_{42}H_{82}N_4S_8Cl_4Re_6$: C, 23.37; H, 3.83; N, 2.60; S, 11.88; Cl, 6.57. Found: C, 22.80; H, 3.62; N, 2.75; S, 11.97; Cl, 6.43. FAB-MASS: $m/z = 1917$ ($M^- - Bu_4N$). ^1H NMR (CD_3CN, 23 °C): δ 7.36 (t, 4H, H_m), 7.92 (t, 2H, H_p), 9.36 (d, 4H, H_o). UV−vis (CH_3CN, nm (ϵ, M^{-1} cm^{-1})): 424 (sh, 1070), 373 (sh, 2400), 306 (sh, 10 400), 270 (sh, 25 100), 240 (sh, 38 300), 226 (52 300).

The third yellow-orange band was eluted with 1:20 acetonitrile/dichloromethane, and the eluate was left for several days to allow for evaporation in air to dryness. The yellow-orange solid was washed with water and a mixed solvent of acetone and ether and then dried in vacuo. Yield of the cis isomer **1b**: 0.080 g (32%). Anal. Calcd: same as for **1a**. Found: C, 24.29; H, 3.39; N, 3.04; S, 11.80; Cl, 6.58. FAB-MASS; $m/z = 1918$ ($M^- - Bu_4N$). ^1H NMR (CD_3CN, 23 °C): δ 7.37 (t, 4H, H_m), 7.94 (t, 2H, H_p), 9.42 (d, 4H, H_o). UV−vis (CH_3CN, nm (ϵ, M^{-1} cm^{-1})): 422 (sh, 1260), 373 (sh, 2390), 303 (sh, 8350), 268 (sh, 16 900), 239 (sh, 39 200), 227 (51 300).

[Bu_4N]$_2$[*trans*-{$Re_6S_8Cl_4$(cpy)$_2$}] (2a) and [Bu_4N]$_2$[*cis*-{$Re_6S_8Cl_4$(cpy)$_2$}] (2b). [Bu_4N]$_3$[$Re_6S_8Cl_6$] (0.300 g, 0.13 mmol) and cpy (0.270 g, 2.6 mmol) were dissolved in 50 mL of DMF. The solution was refluxed for 1 h, and then evaporated to 5 mL under reduced pressure. On addition of 20 mL of water, a brown precipitate was formed, which was collected by filtration. The solid was dissolved in CH_2Cl_2, and the solution was chromatographed on a silica gel column to obtain two geometrical isomers. A red-brown band was held at the top of the column. The first eluate was discarded as it contained only a minor product.

The second red band was eluted with 1:100 C_2H_5OH/dichloromethane, and the eluate was left for several days. The red brown solid deposited was filtered off, washed with water and acetone/ether, and then dried in vacuo. Yield of the trans isomer **2a**: 0.073 g (25%). Anal. Calcd for $C_{44}H_{80}N_6S_8Cl_4Re_6$: C, 23.93; H, 3.65; N, 3.81; S, 11.61; Cl, 6.42. Found: C, 23.80; H, 3.35; N, 3.85; S, 11.93; Cl, 6.46. FAB-MASS: $m/z = 1966$ ($M^- - Bu_4N$). ^1H NMR (CD_3CN, 23 °C): δ 7.61 (d, 4H, H_m), 9.57 (d, 4H, H_o). UV−vis (CH_3CN, nm (ϵ, M^{-1} cm^{-1})): 521 (sh, 310), 320 (11 800), 269 (sh, 27 500), 239 (sh, 41 300), 222 (65 500).

The third red band was eluted with 1:100 C_2H_5OH/dichloromethane, and the eluate was left to dry. The red-brown solid was collected, washed with water and acetone/ether, and then dried in vacuo. Yield of the cis isomer **2b**: 0.080 g (32%). Anal. Calcd: same as **2a**. Found: C, 24.19; H, 3.70; N, 3.71; S, 11.60; Cl, 6.41. FAB-MASS: $m/z = 1967$ ($M^- - Bu_4N$). ^1H NMR (CD_3CN, 23 °C): δ 7.64 (d, 4H, H_m), 9.65 (d, 4H, H_o). UV−vis (CH_3CN, nm (ϵ, M^{-1} cm^{-1})): 529 (sh, 320), 316 (11 800), 240 (sh, 36 000), 223 (64 000).

[Bu_4N][*mer*-{$Re_6S_8Cl_3$(py)$_3$}] (3). [Bu_4N]$_3$[$Re_6S_8Cl_6$] (0.400 g, 0.173 mmol) and py (0.273 g, 3.45 mmol) were dissolved in 64 mL of DMF. The solution was refluxed for 3 d, and was then evaporated to 5 mL under reduced pressure. On addition of 20 mL of water, a yellow-brown precipitate was obtained. The solid was collected by filtration and dissolved in acetonitrile. On allowing the solution to stand for several days, a yellow-orange solid was deposited, which was filtered off, washed with water and a mixture of acetone and ether, and then dried in vacuo. Yield: 0.073 g (22%). Anal. Calcd for $C_{31}H_{51}N_4S_8Cl_3Re_6$: C, 19.00; H, 2.62; N, 2.86; S, 13.09; Cl, 5.43. Found: C, 18.71; H, 2.54; N, 2.76; S, 13.23; Cl, 5.26. FAB-MASS: $m/z = 1717$ ($M^- - Bu_4N$). ^1H NMR (CD_3CN, 23 °C): δ 7.42 (m, 6H, H_m), 7.98 (m, 3H, H_p), 9.38 (d, 4H, H_o), 9.43 (d, 2H, H_o). UV−vis (CH_3CN, nm (ϵ, M^{-1} cm^{-1})): 421 (1050), 374 (sh, 2320), 269 (sh, 24 800), 240 (sh, 36 600), 226 (49 000).

[Bu_4N][*trans*-{Re_6S_8(py)$_2Cl_4$}] (1a′). [Bu_4N]$_2$[*trans*-{$Re_6S_8Cl_4$(py)$_2$}] (**1a**) (0.020 g, 0.0093 mmol) was dissolved in 5 mL of 0.1 M (Bu_4N)PF_6/acetonitrile solution and was electochemically oxidized at a constant potential of 1.2 V vs Ag/AgCl under argon. During the oxidation, a red precipitate was formed, which was collected, washed with acetonitrile and ether, and dried in vacuo. Yield: 0.015 g (85%). Anal. Calcd for $C_{26}H_{46}N_3S_8Cl_4Re_6$: C, 16.30; H, 2.42; N, 2.19; S, 13.39; Cl, 7.40. Found: C, 16.61; H, 2.38; N, 2.59; S, 13.50; Cl, 7.50. ^1H NMR (CD_3CN, 23 °C): δ 8.05 (br, 4H). UV−vis (CH_3CN, nm (ϵ, M^{-1} cm^{-1})): 1408 (370), 545 (1190), 494(890), 269 (sh, 32 000), 252 (38 000), 227 (53 300).

[Bu_4N][*trans*-{$Re_6S_8Cl_4$(cpy)$_2$}] (2a′). [Bu_4N]$_2$[*trans*-{$Re_6S_8Cl_4$(cpy)$_2$}] (**2a**) (0.030 g, 0.014 mmol) was dissolved in 5 mL of 0.1 M (Bu_4N)PF_6/acetonitrile solution and was oxidized electrochemically at a constant potential of 1.2 V vs Ag/AgCl under argon. Ether was diffused to the resulting solution. The red precipitate was formed, which was collected, washed with acetonitrile and ether, and dried in vacuo. Yield: 0.021 g (61%). Anal. Calcd for $C_{28}H_{44}N_5S_8Cl_4Re_6$: C, 17.10; H, 2.26; N, 3.56; S, 13.04; Cl, 7.21. Found: C, 17.10; H, 2.22; N, 3.74; S, 13.20; Cl, 7.17. ^1H NMR (CD_3CN, 23 °C): δ 8.76 (br, 4H, H_m), 16.73 (br, 4H, H_o). UV−vis (CH_2Cl_2, nm (ϵ, M^{-1} cm^{-1})): 1417 (350), 545 (1180), 493 (890), 310 (sh, 14 700), 275 (sh, 30 000), 223 (66 000).

***mer*-[$Re_6S_8Cl_3$(py)$_3$] (3′).** [Bu_4N][*mer*-{$Re_6S_8Cl_3$(py)$_3$}] (**3**) (0.040 g, 0.014 mmol) was dissolved in 30 mL of 0.1 M (Bu_4N)PF_6/acetonitrile solution and was oxidized electrochemically at a constant potential of 1.4 V vs Ag/AgCl under argon. The red-brown precipitate was formed gradually during the electrolysis. The precipitate was collected, washed with acetonitrile and ether, and dried in vacuo. Yield: 0.015 g (56%). Anal. Calcd for $C_{15}H_{15}N_3S_8Cl_3Re_6$: C, 10.49; H, 0.88; N, 2.45; S, 14.93; Cl, 6.19. Found: C, 11.61; H, 1.14; N, 3.26; S, 14.66; Cl, 5.94. ^1H NMR (CD_2Cl_2, 23 °C): δ 7.09 (br, 2H, H_m), 8.03 (br, 4H, H_m), 10.60 (br, 1H, H_p), 10.84 (br, 2H, H_p), 16.49 (br, 2H, H_o), 17.36 (br, 4H, H_o). UV−vis (CH_2Cl_2, nm (ϵ, M^{-1} cm^{-1})): 1380 (360), 547 (1210), 495 (850).

Physical Measurements. UV−vis spectra were recorded on Hitachi U3410 and Hitachi U-3000 spectrophotometers. IR spectra were recorded on a Hitachi 270-50 infrared spectrophotometer. Cyclic voltammetry was performed with a BAS CV-50W voltammetric analyzer and a software package. The working and the counter electrodes were a glassy carbon foil and a platinum wire, respectively. Cyclic voltammograms were recorded at a scan rate of 100 mV/s. The sample solutions (ca. 1 mM) in 0.1 M TBA(PF_6)/acetonitrile were deoxygenated with a stream of argon gas. The reference electrode was Ag/AgCl, against which the half-wave potential of Fc^+/Fc ($E_{1/2}(Fc^{+/0})$ was 0.43 V. Bulk electrolysis was carried out by using a BAS CV-50W voltammetric analyzer with a platinum disk as a working electrode. Magnetic susceptibility data were collected in the temperature range 2.0−300 K in an applied field of 3 T with the use of a Quantum Design Model HPMS SQUID magnetometer. Pascal's constants were used to correct for the diamagnetism of the constituent atoms. The ^1H NMR spectra were obtained at 270.05 MHz with a JEOL JNM-EX 270 spectrometer. All peaks were referenced to the methyl signals of TMS at $\delta = 0$. The temperature was controlled by using an N_2 gas-flow unit consisting of a heating coil immersed in a Dewar of liquid N_2 connected to the NMR tube.

X-ray Structural Determinations. Single crystals of **1a**, **3**, and **2a** were obtained by diffusing ether into the acetonitrile solution, while that of **1a′** was obtained by slow evaporation of the acetonitrile solutions. Crystals of **1a**, **3**, and **1a′** were sealed in glass capillaries, while that of **2a** was mounted on a glass fiber for X-ray measurements. The crystal of **1a** contained two acetonitrile and two water molecules per complex ion. X-ray data for **1a**, **2a**, **3**, and **1a′** were collected at ambient temperature on a Rigaku AFC5R diffractometer with graphite-monochromated Mo Kα radiation. Unit cell parameters were obtained by least-squares refinement of 25 reflections ($25 \le 2\theta \le 30$). None of the crystals showed significant decay throughout the course of data collection. All the data were corrected for Lorentz and polarization effects. Absorption correction (ψ scans) was applied for each compound. Each crystal structure was solved by a direct method (SIR92).[62] The positional and thermal parameters of non-hydrogen atoms except for those of tetra(n-butyl)ammonium cation were refined anisotropically by the full-matrix least-squares method. The C−C bond lengths of tetra(n-butyl)ammonium cations for **1a**, **3**, and **1a′** were fixed at 1.52 Å and refined isotropically. Hydrogen atoms on pyridyl rings were

(62) Altomare, A.; Cascarano, G.; Giacovazzo, C.; Guagliari, A.; Burla, M. C.; Polidori, G.; Camalli, M. *J. Appl. Crystallogr.* **1994**, *27*, 435.

Table 1. Crystallographic Data for $[Bu_4N]_2[trans\text{-}\{Re_6S_8Cl_4(py)_2\}]\cdot 2CH_3CN\cdot 2H_2O$ (**1a**), $[Bu_4N]_2[trans\text{-}\{Re_6S_8Cl_4(cpy)_2\}]$ (**2a**), $[Bu_4N][mer\text{-}\{Re_6S_8Cl_3(py)_3\}]$ (**3**), and $[Bu_4N][trans\text{-}\{Re_6S_8Cl_4(py)_2\}]$ (**1a′**)

	1a·2CH₃CN·2H₂O	**2a**	**3**	**1a′**
empirical formula	$C_{46}H_{92}N_5O_2S_8Cl_4Re_6$	$C_{44}H_{80}N_6S_8Cl_4Re_6$	$C_{31}H_{51}N_4S_8Cl_3Re_6$	$C_{26}H_{46}N_3S_8Cl_4Re_6$
fw	2262.80	2208.69	1959.85	1916.20
T, K	296	296	296	296
λ,Å	0.710 69	0.710 69	0.710 69	0.710 69
cryst syst	monoclinic	orthorhombic	monoclinic	monoclinic
space group	$C2/c$ (no. 15)	$Cmca$ (no. 64)	$P2_1/n$ (no. 14)	$C2/c$ (no.15)
color	yellow-orange	red-brown	yellow-orange	red
Z	4	4	4	4
a, Å	24.693(8)	19.304(3)	16.156(5)	20.524(5)
b, Å	19.464(4)	17.894(7)	19.760(5)	13.794(4)
c, Å	18.592(4)	18.773(4)	18.895(4)	16.399(4)
β, deg	115.76(2)		108.94(2)	109.72(2)
V, Å^3	8047(3)	6484(2)	5705(2)	4370(2)
D_{calcd}, g/cm^3	1.867	2.262	2.281	2.912
μ(Mo Kα), cm^{-1}	93.64	116.17	133.04	174.24
R,^{a} R_w,^{b} %	5.2, 7.7	4.3, 5.1	5.5, 7.3	8.9, 13.4
GOF	1.06	1.05	1.62	1.26

^{a} $R = \sum||F_o| - |F_c||/\sum|F_o|$. ^{b} $R_w = [\sum(|F_o| - |F_c|)^2/\sum w|F_o|^2]^{1/2}$.

Table 2. Selected Bond Distances (Å) and Angles (deg) for $[Bu_4N]_2[trans\text{-}\{Re_6S_8Cl_4(py)_2\}]\cdot 2CH_3CN\cdot 2H_2O$ (**1a**), $[Bu_4N]_2[trans\text{-}\{Re_6S_8Cl_4(cpy)_2\}]$ (**2a**), $[Bu_4N][mer\text{-}\{Re_6S_8Cl_3(py)_3\}]$ (**3**), and $[Bu_4N][trans\text{-}\{Re_6S_8Cl_4(py)_2\}]$ (**1a′**)

	1a	**2a**	**3**	**1a′**
Re−Re	2.5868(9)−2.6007(7)	2.5851(8)−2.6034(6)	2.584(1)−2.604(1)	2.592(2)−2.600(2)
av	2.5930	2.5928	2.594	2.596
Re−S	2.383(3)−2.408(4)	2.391(3)−2.409(3)	2.384(7)−2.415(6)	2.377(9)−2.420(9)
av	2.398	2.400	2.401	2.401
Re−N	2.18(1)	2.21(1)	2.16(2)−2.22(2)	2.16(2)
av			2.19	
Re−Cl	2.425(3), 2.428(3)	2.422(3), 2.424(4)	2.415(7)−2.431(7)	2.401(9), 2.40(1)
av	2.427	2.423	2.424	2.40
Re−Re−Re	89.54(2)−90.46(2)	89.24(3)−90.76(3)	89.48(5)−90.45(5)	89.72(5)−90.28(5)
av	90.00	90.00	90.00	90.00
Re−Re−Re	59.79(2)−60.32(2)	59.72(2)−60.42(1)	59.73(4)−60.34(4)	59.83(5)−60.20(5)
av	60.00	60.00	60.01	60.00
Re−S−Re	65.21(9)−65.75(9)	65.23(7)−65.56(7)	65.0(2)−66.0(2)	65.0(2)−65.8(2)
av	65.44	65.38	65.4	65.5
S−Re−S	172.8(1)−174.1(1)	172.5(1)−174.58(9)	172.2(2)−174.4(2)	172.9(3)−174.0(3)
av	173.3	173.4	173.3	173.3
S−Re−S	89.5(1)−90.3(1)	89.18(9)−90.35(9)	89.0(2)−90.7(2)	88.9(3)−90.9(3)
av	89.8	89.8	89.8	89.8
Re−Re−N	133.8(4)−135.8(4)	134.62(1)−134.9(3)	132.8(5)−137.3(5)	132.6(8)−137.7(8)
av	134.8	134.7	134.9	135.1
Re−Re−Cl	134.6(1)−135.6(1)	134.94(1)−135.5(1)	134.3(2)−136.1(2)	133.7(2)−136.1(2)
av	135.1	135.22	135.1	135.0

included at calculated positions with fixed displacement parameters (1.2 times the displacement parameters of the attached carbon atom). All calculations were performed using TEXSAN.[63] Crystallographic data are listed in Table 1. Selected bond lengths and angles are listed in Table 2. Non-hydrogen atom coordinates, anisotropic thermal parameters, and a full listing of bond distances and angles for **1a**, **2a**, **3**, and **1a′** are included as Supporting Information.

Result and Discussion

Preparation of Pyridine-Coordinated Re_6S_8 Clusters. A series of octa(μ_3-sulfido)hexarhenium(III) clusters with mixed chloride−pyridine terminal ligands $[Re_6S_8Cl_{6-n}(py)_n]^{(4-n)-}$ (n = 2−4) have been prepared from the one-electron-oxidized species $[Re_6S_8Cl_6]^{3-}$ (reported as $[Re_6S_7(SH)Cl_6]^{3-}$ previously (vide infra))[38] by slow ligand substitutions and spontaneous reduction. The reduction step becomes favorable on coordination of pyridine as indicated by the redox potentials (vide infra). The ratio of chloride to pyridine was controlled by the amount of pyridine and time for refluxing. The successful control is based on the extremely inert nature of the Re_6S_8 center for terminal ligand substitution.[64,65] Several reaction products containing different numbers of coordinated pyridines and geometrical isomers were formed under the various conditions employed, as found by ^{1}H NMR spectra of the reaction mixture. Products of the reaction mixtures were effectively separated into each complex by using silica gel chromatography. For example, when $[Re_6S_8Cl_6]^{3-}$ and 20 equiv of pyridine were refluxed for 1 h in DMF, cis and trans isomers of doubly substituted pyridine complexes (n = 2) were produced as major products. The two geometrical isomers were separated by silica gel column chromatography by using dichloromethane/acetonitrile (20:1 v/v) as an eluent. The yields of the cis and trans isomers were almost the same, which is compared with the case of $[Re_6S_8Br_4(PEt_3)_2]^{2-}$ where the trans isomer was a major product.[44] In the case of the cpy complexes, separation of the reaction mixtures was done by using dichloromethane/C_2H_5OH (100:1 v/v) as an eluent.

For the trisubstituted complexes, the mer isomer of $[Re_6S_8Cl_3(py)_3]^-$ was obtained as a major product. The tetrasubstituted complex, $Re_6S_8Cl_2(py)_4$ was obtained by using 400 equiv of pyridine with a prolonged refluxing time. $[Bu_4N]_3[Re_6S_8Cl_6]$ (0.100 g, 0.043 mmol) and py (1.36 g, 17.2 mmol) were

(63) *TEXSAN. Single-Crystal Structure Analysis Package*; Molecular Structure Corp.: Woodlands, TX, 1992.
(64) Fedin, V. P.; Virovets, A. A.; Sykes, A. G. *Inorg. Chim. Acta* **1998**, *271*, 228−230.
(65) Fedin, V. P.; Yoshimura, T.; Sasaki, Y.; Sykes, A. G. Unpublished results.

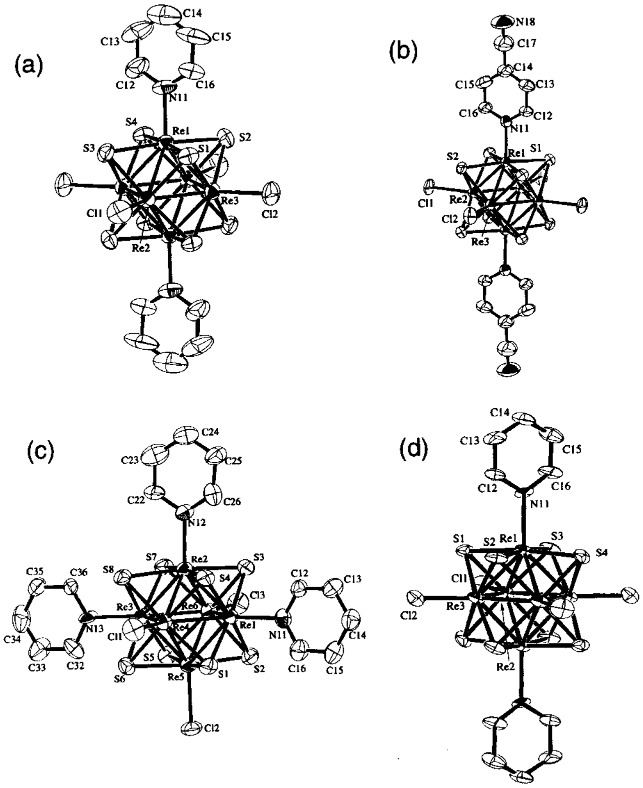

Figure 1. ORTEP drawings showing the complex anion and numbering scheme for (a) $[Bu_4N]_2$[*trans*-$\{Re_6S_8Cl_4(py)_2\}$] (**1a**), (b) $[Bu_4N]_2$[*trans*-$\{Re_6S_8Cl_4(cpy)_2\}$] (**2a**), (c) $[Bu_4N]$[*mer*-$\{Re_6S_8Cl_3(py)_3\}$], and (d) $[Bu_4N]$[*trans*-$\{Re_6S_8Cl_4(py)_2\}$] (**1a′**). Ellipsoids are drawn at the 50% probability level. The hydrogen atoms have been omitted for clarity.

dissolved in 10 mL of DMF. The solution was refluxed for 4 d. The yellow-orange precipitate formed was filtered off, washed with acetonitrile, water, and ether, and then dried in vacuo (yield 0.014 g, 17%). The low solubility of the neutral tetra(pyridine) species, which is clearly demonstrated by the lack of IR bands of tetra-*n*-butylammonium cation, prevents us from separating the products into two possible geometrical isomers. The substitution reaction of pyridine at the terminal sites was slower than that of PEt_3 for the bromide ligands in $[Re_6S_8Br_6]^{4-}$.[44] The stronger donor ability of PEt_3 and easier dissociation of Br^- as compared with Cl^- may be responsible for the difference.

Preparation of One-Electron-Oxidized Re_6S_8 Clusters. The one-electron-oxidized species have been prepared by the electrolysis at constant potentials of 1.2 V (**1a′** and **2a′**) and 1.4 V (**3′**) vs Ag/AgCl in acetonitrile. The complexes **1a′** and **3′** were precipitated during the electrolysis because of the low solubility of **1a′** and **3′** in acetonitrile. The oxidized clusters **1a′** and **3′** are only sparingly soluble in acetonitrile and in dichloromethane, respectively. On the contrary diffusion of ether to the electrolyzed solution was required to obtain a solid sample of **2a′**. The electrolytic oxidation of **1b** was carried out in acetonitrile, but the product was not isolated because of its high solubility.

Structures of Pyridine-Coordinated Re_6S_8 Clusters. The molecular geometry and labeling scheme of **1a**, **2a**, **3**, and **1a′** are shown in Figure 1. The central octahedral unit of six Re atoms with eight S atoms capping metal triangle faces are common features for all four complexes. The terminal positions are occupied by pyridine or 4-cyanopyridine and chloride ions. **1a** and **2a** have a centrosymmetric configuration, while **3** has no crystallographic molecular symmetry. The two pyridine and 4-cyanopyridine ligands occupy mutually trans positions for **1a** and **2a**, respectively. For **3** three pyridines are arranged in a mer configuration.

The Re−Re bond distances span the range 2.5868(9)−2.6007(7) Å for **1a**, 2.5851(8)−2.6034(6) Å for **2a**, and 2.584(1)−2.604(1) Å for **3** (Table 2). No appreciable difference in the distances is seen in the three complexes, so the cyano group of cpy is not influential structurally nor is the number of pyridine ligands. The average value of the Re−Re distance is similar to those of $[Re_6S_8X_6]^{4-}$ (X^- = halide ion) and $[Re_6S_8Br_{6-n}(PEt_3)_n]^{(4-n)-}$.[38,44] It seems that the difference in the terminal ligands does not significantly influence the structure of the Re_6 core. The Re−Cl distance (2.425(3) and 2.428(3) Å for **1a**, 2.422(3) and 2.424(4) Å for **2a**, and 2.415(7), 2.426(6), and 2.431(7) Å for **3**) are also similar to those (2.448(10)−2.457(9) Å) in $[Re_6S_8Cl_6]^{4-}$. The Re^{III}−N(py) distances (2.16(2)−2.22(2) Å) of the clusters are longer than those of mononuclear rhenium(III) complexes $ReCl(HBpz_3)(OPh)(py)\cdot C_6D_6$ (2.146(4) Å) ($HBpz_3$ = hydrogen tris(pyrazolyl)borane),[66] *mer*-$[ReCl_3(py)_3]$ (2.116(5)−2.120(8) Å),[67] and $[Bu_4N]$[*trans*-$\{ReBr_4(py)_2\}$] (2.120(5) and 2.154(4) Å).[67]

The structure of **1a′** represents the oxidized species $Re^{III}_5Re^{IV}$. Previously reported structures of the protonated species[38] are very similar to that of **1a′** with respect to the hexarhenium cluster core. As was discussed in the previous section, these structures may in fact represent one-electron-oxidized species. Structural studies of other hexanuclear cluster complexes indicated that the metal−metal distance decreases with increasing oxidation states as shown in Co and Fe complexes,[68] and less extensively in Mo and W complexes.[68] The Re−Re distance of **1a′** is almost the same as that of **1a**. The Re−Re bonds in the Re^{III}_6 clusters are considered as formal single bonds since Re^{III} has four d-electrons. The change in formal bond order on oxidation to $Re^{III}_5Re^{IV}$ is small, from 1 to 0.96, which may explain the fact that there is no appreciable change in the Re−Re distance between **1a** and **1a′**. An increased oxidation state in **1a′** is reflected in shorter Re−Cl (2.401(9) and 2.40(1) Å) distances **1a′** as compared with those in **1a** (2.425(3) and 2.428(3) Å). A similar trend is seen in the M−P(PEt_3) distances of other hexametal clusters (M = Co, Fe).[68] It is interesting that the trend is in the reverse direction in the Mo and W clusters.[68] Other bond distances and angles for **1a′** are nearly the same as the corresponding values for **1a**.

^{1}H NMR Measurements. ^{1}H NMR spectra of all the new cluster complexes were measured in CD_3CN at room temperature. The chemical shifts are given in the Experimental Section and in Table S1 in the Supporting Information. The proton signals of py or cpy ligands of the Re^{III}_6 complexes **1a**, **1b**, **2a**, **2b**, and **3** show a downfield shift relative to those of the free ligands, suggesting that the ligands are not dissociated in solution. The *ortho*-proton (H_o) signals of **3** have two different resonances with an integral intensity ratio of 2:1, suggesting the mer configuration of the complex. It is seen that the pyridine protons trans to another pyridine resonate at upper field relative to those of the pyridine protons trans to Cl^-, as the comparative signals of **1a** and **1b** (and **2a** and **2b**) and also two signals of the mer isomer **3** show.

The ^{1}H NMR signals of pyridyl protons of one-electron-oxidized complexes **1a′**, **2a′**, and **3′** appear at lower field beyond the regions of diamagnetic complexes with considerable broadening (Figure S1 in the Supporting Information). The chemical

(66) Brown, S. N.; Mayer, J. M. *Organometallics* **1995**, *14*, 2951−2960.
(67) Arp, O.; Preetz, W. *Z. Anorg. Allg. Chem.* **1996**, *622*, 219−224.
(68) Goddard, C. A.; Long, J. R.; Holm, R. H. *Inorg. Chem.* **1996**, *35*, 4347−4354.

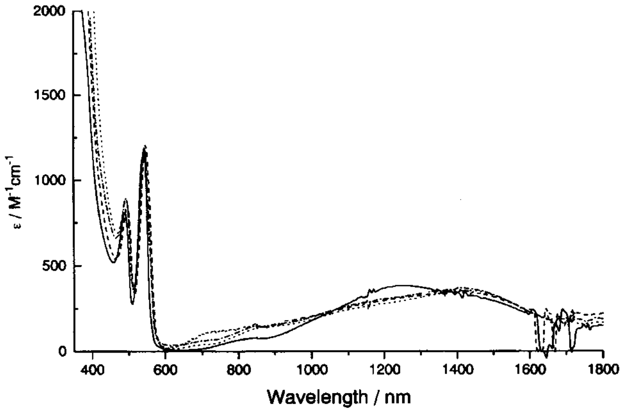

Figure 2. Visible and near-infrared spectra for the one-electron-oxidized complexes $[Re_6S_8Cl_6]^{3-}$ in CH_3CN (solid line), *trans*-$[Re_6S_8Cl_4(py)_2]^-$ in CH_3CN (dashed−dotted line), *trans*-$[Re_6S_8Cl_4(cpy)_2]^-$ in CH_2Cl_2 (dotted line), and *mer*-$[Re_6S_8Cl_3(py)_3]$ in CH_2Cl_2 (dashed line).

shifts may be taken as additional evidence for the oxidation state of these complexes with one unpaired electron. The signal assignments were made by using the solutions containing the redox pairs, **1a** and **1a′**, **2a** and **2a′**, and **3** and **3′**. The pairs of signals show temperature-dependent coalescent behavior, so the assignment can be made unambiguously. All the signals show a temperature-dependent shift, lower field at lower temperatures. The H_o signals of pyridine or 4-cyanopyridine exhibit the strongest influence of paramagnetism of $Re^{III}{}_5Re^{IV}$. The H_o signals for **2a′** (16.73 ppm) and **3′** (16.49 and 17.36 ppm) at room temperature in CD_2Cl_2 shift to 23.18, and 22.54 and 24.04 ppm at −90 °C, respectively. The tris(pyridine) complex **3′** shows two kinds of pyridine proton resonances with a 2:1 integrated intensity ratio (Figure S1), suggesting that the mer-configuration is retained on oxidation. The signals of the countercation n-Bu_4N^+ are unaffected by the paramagnetism of the cluster core, showing sharp and well resolved signals at nearly the same position as those of the unoxidized diamagnetic species.

UV−Vis Absorption Spectra. UV−vis absorption spectra of the new $Re^{III}{}_6$ and $Re^{III}{}_5Re^{IV}$ complexes were measured in acetonitrile at room temperature (Table S2 and Figure S2 in the Supporting Information). All the $Re^{III}{}_6$ complexes show featureless spectral patterns in the region >300 nm. In both bis(py) and bis(cpy) complexes, cis isomers exhibit a distinctive shoulder or a peak at ca. 320 nm. The trans isomers have a distinctive shoulder at ca. 270 nm, the intensity of which is nearly twice that of the cis isomers. The absorption band at ca. 320 nm found in cis isomers seems to be obscured by this strong absorption in the trans isomers. The spectrum of **3** is similar to that of the *cis*-bis(py) isomer with respect to the intense absorption shoulder at ca. 270 nm, which seems to be due to the partial *trans*-pyridine structure in **3**. This feature seems to depend on the kind of pyridine derivative ligands, and is not found clearly for the 4-methylpyridine and pyrazine complexes.

The UV−vis absorption spectra of one-electron-oxidized complexes **1a′**, **2a′**, and **3′** are very similar in shape to one another (Figure 2). The spectrum of **1b′** was obtained in situ by the spectroelectrochemical technique. No significant difference was observed between the spectra of *trans*- and *cis*-bis(py) complexes **1a′** and **1b′**. Three absorption peaks are observed in the near-infrared and visible regions. The weak absorption band at ca. 1410 nm is also noted, which is ascribed to the intervalence transition (IT band) of the mixed-valence state $Re^{III}{}_5Re^{IV}$. The band is not observed in the $Re^{III}{}_6$ complexes.

Table 3. Redox Potentials of the New Complexes in 0.1 M $(Bu_4N)PF_6/CH_3CN$[a]

	$E_{1/2}$/V, vs Ag/AgCl (ΔE_p[b])		
	$Re^{III}{}_6$/ $Re^{III}{}_5Re^{IV}$	$Re^{III}{}_5Re^{IV}$/ $Re^{III}{}_4Re_2{}^{IV}$	ligand (cpy^-/cpy)
$[Re_6S_8Cl_6]^{4-}$ [c]	+0.31 (70)	+1.17 (90)[d]	
1a	+0.77 (70)		
1b	+0.77 (70)		
2a	+0.83 (60)		−1.19, −1.28
2b	+0.83 (60)		−1.18, −1.29
3	+0.97 (70)		

[a] $E_{1/2} = (E_{pa} + E_{pc})/2$, where E_{pa} and E_{pc} are anodic and cathodic peak potentials, respectively. [b] $\Delta E_p = E_{pa} - E_{pc}$. [c] The $Re^{III}{}_6/Re^{III}{}_5Re^{IV}$ process of $[Re_6S_8Cl_6]^{4-}$ has already been reported by R. H. Holm and co-workers,[38] but second redox process has not been reported. [d] Quasi-reversible process.

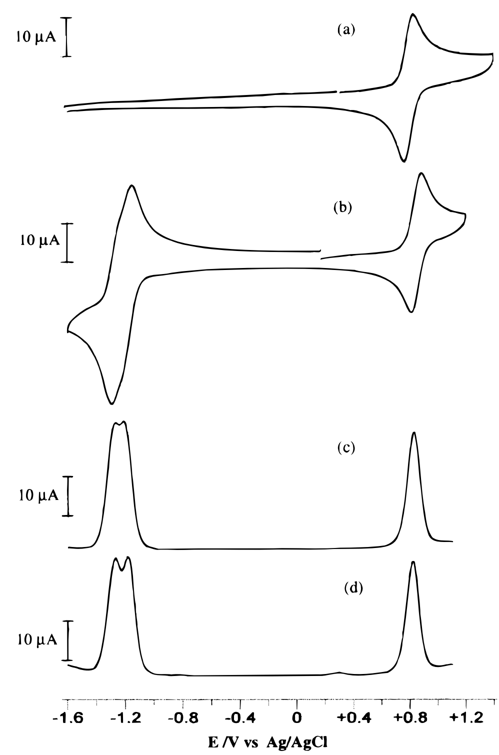

Figure 3. Cyclic voltammograms of $[Bu_4N]_2[$*trans*-$\{Re_6S_8Cl_4(py)_2\}]$ (a) and $[Bu_4N]_2[$*trans*-$\{Re_6S_8Cl_4(cpy)_2\}]$ (b) and differential pulse voltammograms of $[Bu_4N]_2[$*trans*-$\{Re_6S_8Cl_4(cpy)_2\}]$ (c), and $[Bu_4N]_2[$*cis*-$\{Re_6S_8Cl_4(cpy)_2\}]$ (d) in a 0.1 M $(Bu_4N)PF_6-CH_3CN$ solution. Scane rate 100 mV/s for cyclic voltammetry and 20 mV/s for differential pulse voltammetry.

The spectra are reminiscent of that reported for the protonated complex $[Re_6S_7(SH)Cl_6]^{3-}$.[38]

Electrochemical Studies. Electrochemical properties of the new Re_6 complexes in acetonitrile were studied by cyclic and differential pulse voltammetries at room temperature. The redox potentials are summarized in Table 3. Cyclic and differential pulse voltammograms of the bis(py) and bis(cpy) complexes are shown in Figure 3. All the complexes show a reversible one-electron oxidation wave in the region +0.77 to +0.97 V vs Ag/AgCl. The one-electron nature of the waves was confirmed by coulometry. Two complexes of the redox pair **1a** and **1a′** give identical CV; so do other redox pairs. Table 3 also includes the potentials of $[Re_6S_8Cl_6]^{4-}$.[68] In addition to the one-electron oxidation wave, the potential of which is in excellent agreement with the one reported by Holm and co-workers,[38] we have observed a second oxidation wave at 1.17 V ($Re^{III}{}_5Re^{IV}/Re^{III}{}_4Re^{IV}{}_2$), which was not reported previously.

The new pyridine-containing complexes do not show the second oxidation wave up to 1.50 V.

The one-electron oxidation potentials of the pyridine complexes are significantly more positive than that of $[Re_6S_8Cl_6]^{4-}$, indicating that the net charge of the Re_6 complexes may be important as the pyridine complexes have less negative charge, so the oxidation is less favorable. The second oxidation waves of the py and cpy complexes may also be positively shifted to outside of the measured potential range. The redox potentials depend linearly on the pK_a of a series of pyridyl ligands including py and cpy.[69]

The geometrical isomerism does not appear to give any significant influence on the Re_6 core oxidation since **1a** and **1b**, and **2a** and **2b**, are oxidized at the same potentials. The comparison of the data of **1a** and **2a** (also **1b** and **2b**) indicated that the cpy complexes are more difficult to be oxidized by 0.06 V, reflecting the difference in the basicity of the ligands.

The cpy complexes showed additional redox waves at −1.19 and −1.28 V for **2a** and −1.18 and −1.29 V for **2b** vs Ag/AgCl (Figure 3c,d). These waves are ascribed to the ligand-centered reduction cpy/cpy$^-$, since no corresponding waves are observed for **1a** and **1b**. It should be noted that the cpy/cpy$^-$ process splits into two with a 1:1 current intensity ratio as Figure 3 shows. The ligand-based redox potentials and the extent of the splitting are essentially independent of the geometrical isomerism, cis and trans. Two factors are considered for the splitting of the ligand-reduction waves: (1) electrostatic repulsions between the two ligands and (2) cluster-mediated ligand−ligand electronic interactions. Since the electrostatic repulsion may not be significant in the present case with the large cluster core, the splitting would be more likely to be due to cluster-mediated ligand−ligand electronic interactions.

Magnetic Properties. Temperature-dependent magnetic susceptibilities for the complexes **1a′**, **3′**, and **3** were measured over the temperature range of 2−300 K at 5 K intervals in a field of 3 T using a SQUID. The data were corrected for diamagnetic core contributions using Pascal's constants for individual ions. The molar susceptibility data for **3** (Figure S3 in the Supporting Information) show the existence of a small amount of paramagnetic component, which is very low even at lower temperatures. It is not definite whether the paramagnetic component is due to the existence of a small amount of impurity or due to intrinsic magnetism from the hexanuclear Re^{III} assembly. Even if the latter is the case for the hexanuclear Re^{III} system, the paramagnetic contribution is very small and the Re^{III}_6 complex **3** is regarded as essentially diamagnetic with all the d electrons (24e) effectively coupled within the Re_6 core. The temperature dependence of the magnetic susceptibility of **3′** has a large value at lower temperature, and shows typical paramagnetic behavior (Figure S3). Similar behavior was observed for **1a′**. The plots of the reciprocal molar susceptibility for **1a′** and **3′** are shown in Figure 4. The data of **3′** can roughly fit the Curie−Weiss relationship, $X_M = C/(T - \Theta)$ from the data in the temperature range 2−300 K. The μ_{eff} value was estimated to be 2.1 μB, which is somewhat larger than the value for the spin-only d^1 electron per cluster unit (1.73 μB). The ground state of the cluster **3′** was regarded as $S = 1/2$ per cluster unit. Similar behavior was observed for **1a′** (2−80 K), and its ground state is also $S = 1/2$, although the Curie−Weiss relationship did not hold at higher temperature in this complex. The reason for the deviation from the relationship was not clear at the present stage.

(69) Yoshimura, T.; Umakoshi, K.; Sasaki, Y.; Ishizaka, S.; Kim, H.-B.; Kitamura, N. Submitted for publication.

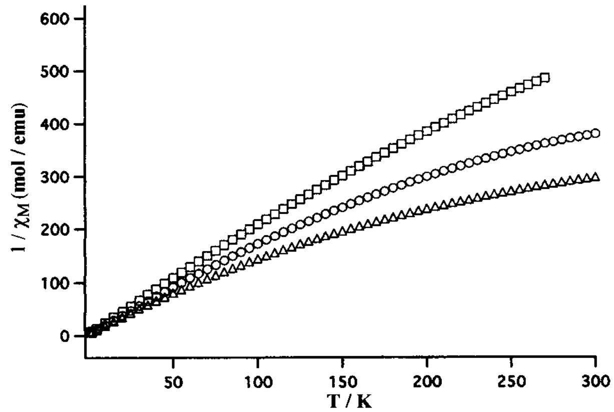

Figure 4. Temperature dependencies of the reciprocal molar magnetic susceptibilities of $[Bu_4N]_3[Re_6S_8Cl_6]$ (open triangles), $[Bu_4N][$*trans*-$\{Re_6S_8Cl_4(py)_2\}]$ (**1′**), (open circles), and *mer*-$[Re_6S_8Cl_3(py)_3]$ (**3′**) (open squares).

Electron Self-Exchange between $[Re_6S_8Cl_4(cpy)_2]^{2-}$ and $[Re_6S_8Cl_4(cpy)_2]^{-}$. As mentioned in the ^{1}H NMR section, when the Re^{III}_6 complex and its one-electron-oxidized species are mixed in CD_2Cl_2 solution, signals from the two complexes which appear separately at low temperature start to coalesce as the temperature is raised. From the analysis of the temperature-dependent coalescence behavior, it is possible to evaluate electron self-exchange rate constants for the reaction between the two species. The analysis was applied for the redox pair **2a** and **2a′** by using H_m proton signals. Figure 5 shows the spectra of the H_m signal, the left-hand side being the spectra at various temperatures and the right-hand side being its computer-simulated best-fit spectra. For the simulation, a computer program based on the modified Bloch equation for the two-site exchange was used.[70] The two chemical shifts and their half-widths of the individual species at each temperature were taken from the spectra of individual species, and the spectrum of the fast-exchange limit was obtained at >−40 °C. At even the lowest temperature, −90 °C, the slow-exchange limit was not reached. The second-order rate constants thus obtained by computer simulation are listed in Table 4. The Eyring plot (Figure S4 in the Supporting Information) displays a good straight line, from which the activation parameters were estimated as $\Delta H^{\ddagger} = 30.2 \pm 2.1$ kJ mol^{-1} and $\Delta S^{\ddagger} = 30 \pm 8$ J K^{-1} mol^{-1}. The second-order rate constant at 298.2 K obtained by using these parameters is 1.2×10^9 M^{-1} s^{-1}. The value is among the largest outer-sphere self-exchange rate constants ever measured. The small structural difference between $[Bu_4N]_2[$*trans*-$\{Re_6S_8(py)_2Cl_4\}]$ (**1a**) and its one-electron-oxidized species **1a′** indicates that small structural reorganization energy would be required on the electron self-exchange between the analogous couple **2a** and **2a′**. Also, because of the rather large size of the hexarhenium cluster, a small change in solvation between the two redox states is expected. Relatively small $\Delta H^{\ddagger}$ and mildly positive $\Delta S^{\ddagger}$ values seem to be consistent with rather small structural and solvation reorganization energies. Similar large self-exchange rate constants have been reported recently for $[Re_2X_4(PMe_2Ph)_4]^{0/+}$ ($X^- = Cl^-$, 2.5×10^8 M^{-1} s^{-1}; $X^- = Br^-$, 4.2×10^8 M^{-1} s^{-1} at 298 K) in CD_2Cl_2.[71] The intramolecular electron-exchange rate constant for the mixed-valence "dimer" of the trinuclear ruthenium complex [{Ru$_3$-

(70) Sandstrom, J. *Dynamic NMR Spectroscopy*; Academic Press Inc. Ltd.: London, 1982.

(71) Coddington, J.; Wherland, S. *Inorg. Chem.* **1997**, *36*, 6235−6237.

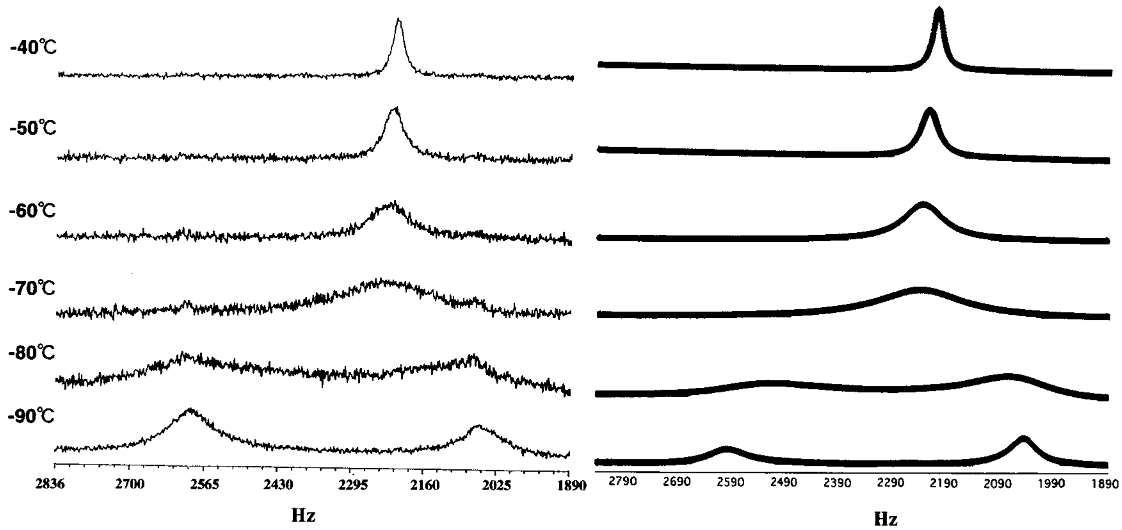

Figure 5. Variable-temperature ^{1}H NMR spectra for a mixture of 0.73 mM $[Bu_4N]_2[trans\text{-}\{Re_6S_8Cl_4(cpy)_2\}]$ (**2a**) and 0.55 mM $[Bu_4N][trans\text{-}\{Re_6S_8Cl_4(cpy)_2\}]$ (**2a′**) in CD_2Cl_2 (left) and computer-simulated spectra (right). The range of 2500−2700 Hz in the ^{1}H NMR spectra is for the H_o signal of diamagnetic $[Bu_4N]_2[trans\text{-}\{Re_6S_8Cl_4(cpy)_2\}]$ overlapped with the H_m signal of paramagnetic $[Bu_4N][trans\text{-}\{Re_6S_8Cl_4(cpy)_2\}]$ at −80 and −90 °C.

Table 4. Second-Order Rate Constants for the Self-Exchange Reaction between $[Bu_4N]_2[trans\text{-}\{Re_6S_8Cl_4(cpy)_2\}]$ (**2a**) and $[Bu_4N][trans\text{-}\{Re_6S_8Cl_4(cpy)_2\}]$ (**2a′**) in CD_2Cl_2

	T 233 K	*T* 223 K	*T* 213 K	*T* 203 K	*T* 193 K	*T* 183 K
$10^{-5}k$, $M^{-1}\,s^{-1}$ [a]	260	160	65	36	9.8	3.1
$10^{-5}k$, $M^{-1}\,s^{-1}$ [b]	210	140		28		3.4

[a] **2a**, 0.73 mM; **2a′**, 0.55 mM. [b] **2a**, 1.45 mM, **2a′**, 0.64 mM.

$(\mu_3\text{-}O)(\mu\text{-}CH_3COO)_6(CO)(py)\}_2(\mu\text{-pyrazine})]^+$ has also been determined as $5.3 \times 10^{11}\ s^{-1}$.[72]

Nature of $[Re_6S_7(SH)Cl_6]^{3-}$ and Analogues. During the study, we noticed that the electronic absorption spectra of the one-electron-oxidized species **1a′**, **2a′**, and **3′** are very similar to that reported for $[Re_6S_7(SH)Cl_6]^{3-}$.[37] From magnetic measurements described below, we now believe that the reported "protonated species" is in fact the one-electron-oxidized species $[Re_6S_8Cl_6]^{3-}$. We have measured the spectrum of the "protonated complex" and found an intervalence absorption peak at 1254 nm in addition to the visible band at 489 and 544 nm in acetonitrile. Temperature-dependent magnetic susceptibilities (2−80 K) for the tetra(*n*-butyl)ammonium salt of the complex leave a large value at lower temperature, and show typical paramagnetic behavior. The plot of the reciprocal molar susceptibility shown in Figure 4 indicated that the complex has a ground state of $S = 1/2$. Other so-called protonated species such as $[Re_6Se_7(SeH)Cl_6]^{3-}$ have to be reexamined with regard to their composition.

Conclusions

A series of face-capped octahedral octa(μ_3-sulfido)hexarhenium(III) clusters having mixed Cl−py or Cl−cpy ligands, $[Re_6S_8Cl_{6-n}(\text{py or cpy})_n]^{(4-n)-}$ ($n = 2-4$), including cis and trans geometrical isomers for $n = 2$, and three of their one-electron-oxidized species have been prepared. Four of them have been X-ray structurally characterized. Structural comparison of $[trans\text{-}\{Re_6S_8Cl_4(py)_2\}]^{2-}$ and its one-electron-oxidized species $[trans\text{-}\{Re_6S_8Cl_4(py)_2\}]^{-}$ shows no significant change in structural parameters. The electron self-exchange rate constant between $[trans\text{-}\{Re_6S_8Cl_4(cpy)_2\}]^{2-}$ and $[trans\text{-}\{Re_6S_8Cl_4(cpy)_2\}]^{-}$ has been evaluated to be $1.2 \times 10^9\ M^{-1}\ s^{-1}$ (298.2 K). Oxidized species have been further characterized by magnetic measurements to have an $S = 1/2$ ground state. We have found that the hexarhenium(III) complexes are strongly luminescent at room temperature both in the solid state and in solution.[61,73] Successful stepwise substitution of terminal chloride ligands of $[Re_6S_8Cl_6]^{4-}$ by py and cpy can be applied to other pyridine derivative ligands to produce various interesting complexes based on the hexarhenium clusters, and work along these lines is already in progress.

Acknowledgment. Grants-in-Aid Nos. 09237106 and 10149102 (Priority Areas of "Electrochemistry of Ordered Interface" and "Metal-Assembled Complexes") and the International Scientific Research Program between Hokkaido University and The University of Newcastle-upon-Tyne (Grant No. 08044046) from Ministry of Education, Science, Sports and Culture, Japan, are gratefully acknowledged. We thank Professor Y. Hinatsu and Dr. A. Wakeshima of Hokkaido University for magnetic measurements.

Supporting Information Available: Tables of ^{1}H NMR and electronic absorption spectral data, figures of the ^{1}H NMR spectra of **3** and **3′**, UV−vis spectra of **1a** and **1b**, temperature dependence of the magnetic susceptibility of **3** and **3′**, and Eyring plot for the self-exchange reaction between **2a** and **2a′**, and X-ray crystallographic files in CIF format for the structure determinations of **1a**, **2a**, **3**, and **1a′**. This material is available free of charge via the Internet at http://pubs.acs.org.

IC9907922

(72) Ito, T.; Hamaguchi, T.; Nagino, H.; Yamaguchi, T.; Washington, J.; Kubiak, C. P. *Science* **1997**, *277*, 660−663.
(73) Yoshimura, T.; Ishizaka, S.; Sasaki, Y.; Kim, H.-B.; Kitamura, N.; Naumov, N. G.; Sokolov, M. N.; Fedorov, V. E. *Chem. Lett.* **1999**, 1121−1122.